Electrical and Rheological Percolation in Polystyrene/MWCNT Nanocomposites

Arun K. Kota,[†] Bani H. Cipriano,[‡] Matthew K. Duesterberg,[§] Alan L. Gershon,[†] Dan Powell,[§] Srinivasa R. Raghavan,[‡] and Hugh A. Bruck*,[†]

Departments of Mechanical and Chemical and Biomolecular Engineering, University of Maryland, College Park, Maryland 20742, and NASA-Goddard Space Flight Center, Greenbelt, Maryland 20771

Received May 24, 2007; Revised Manuscript Received July 16, 2007

ABSTRACT: A systematic electrical and rheological characterization of percolation in commercial polydisperse polystyrene (PS) nanocomposites containing multiwall carbon nanotubes (MWCNTs) is presented. The MWCNTs confer appreciable electrical conductivities (up to ca. 1 S/m) to these nanocomposites at a concentration of 8 vol %. In addition to enhancing the electrical properties, even at small concentrations (ca. 2 vol %), MWCNTs significantly enhance the rheological properties of PS melts. At concentrations exceeding 2 vol %, a plateau appears in the storage modulus G' at low frequencies, indicating the formation of a percolated MWCNT network that responds elastically over long timescales. Network formation, in turn, implies a diverging complex viscosity vs complex modulus curve. A focus of this study is on the correlation between electrical and rheological properties at the onset of percolation. The experimental results indicate that the elastic load transfer and electrical conductivity are far more sensitive to the onset of percolation than the viscous dissipation in the nanocomposite. Sensitivity of the electrical and rheological percolations to two different solvents used in processing the nanocomposites has also been characterized.

1. Introduction

Polymer nanocomposites based on carbon nanotubes (CNTs) are attracting attention due to their remarkable mechanical, thermal, and electrical properties. The high aspect ratio of CNTs allows property enhancement at lower concentrations[1] as compared to conventional particles such as carbon black or nanoclays. The motivation for the present work is the potential use of polymer/CNT nanocomposites as conductive, strong, and yet lightweight materials in the civilian space arena (e.g., as radiation shielding materials). In this study, multiwalled carbon nanotubes (MWCNTs), ∼150−200 nm in diameter and ∼5−10 μm in length, which have commercial viability were employed. The MWCNTs are added as fillers to commercial polydisperse polystyrene (PS), which has potential applications in radiation shielding due its relatively high content of hydrogen. The resulting PS/MWCNT nanocomposites are processed from solution using two different solvents, dimethylformamide (DMF) and tetrahydrofuran (THF), which have been previously determined to be suitable for processing of PS.[2] The nanocomposites were subsequently characterized for their electrical conductivity and rheological properties. These techniques together provide insight into the nanoscale structure and organization of the MWCNTs in the PS matrix.

PS/CNT nanocomposites have been recently studied in a few research investigations. Qian et al.[3,4] fabricated PS/MWCNT films by solvent evaporation and reported a 42% increase in the elastic modulus due to the particles. Thostenson et al.[5] utilized solvent evaporation followed by microscale twin screw extrusion to obtain highly aligned PS/MWCNT films that exhibited a 49% increase in elastic modulus. Andrews et al.[1] produced PS/MWCNT nanocomposites via melt mixing and reported a good dispersion with an electrical percolation at 0.25 vol %. Safadi et al.[6] prepared PS/MWCNT films via spin-casting and reported a transformation from insulating to conducting and a 100% increase in the tensile modulus at 5 wt %. Finally, Mitchell et al.[7] added functionalized single-wall carbon nanotubes (SWCNTs) to PS and studied the melt rheology of the nanocomposites, and demonstrated the presence of a percolated network of SWCNTs at concentration exceeding 1.5 wt %.

To date, the melt rheology of PS/MWCNT nanocomposites has not been thoroughly investigated. Systematic rheological studies have been conducted, however, for MWCNT nanocomposites based on polycarbonate (PC),[8,9] polyethylene (PE),[10] and polymethyl methacrylate (PMMA).[11] Also, while the conductivity[11−16] and rheological properties[11,15−17] of polymer/CNT nanocomposites have been studied independently, no attempts have been made to correlate these two sets of properties. It should be noted that both properties fundamentally depend on the degree of percolation in the nanocomposite. In this paper, a systematic investigation is presented that characterizes the evolution of electrical conductivity and melt rheology of solvent processed PS/MWCNT nanocomposites as the filler concentration is varied. Furthermore, the effect that two different solvents have on the evolution of these properties is also studied. The focus of this research investigation is to elucidate on the interrelationship between electrical conductivity and various rheological properties at the onset of percolation in these nanocomposites.

2. Experimental Section

2.1. Ingredients and Processing. Similar to previous research investigations,[11,18] a polymer well-suited for solvent processing and fundamental melt rheology investigations, a commercial polydisperse PS (weight-average molecular weight ∼150 000, polydispersity ∼2.73, density ∼1.04 g/cm^3) from Nova Chemicals, was used as the matrix material. Vapor grown, graphitized MWCNTs (diameter ∼ 150−200 nm, length ∼ 5−10 μm, density ∼ 0.6 g/cm^3) obtained from the University of Kentucky, Lexington, KY, were used as the filler (see Figure 1). A detailed account of the synthesis,

* Corresponding author. E-mail: bruck@eng.umd.edu.
[†] Department of Mechanical Engineering, University of Maryland.
[‡] Department of Chemical and Biomolecular Engineering, University of Maryland.
[§] NASA-Goddard Space Flight Center.

10.1021/ma0711792 CCC: $37.00
Published on Web 09/08/2007

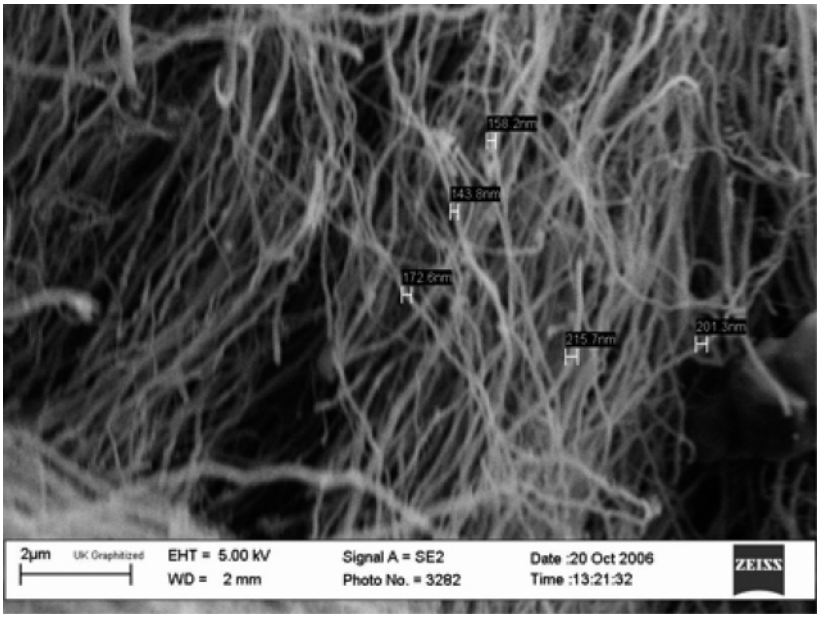

Figure 1. SEM micrograph of MWCNTs used in this investigation, obtained from University of Kentucky.

purification, and characterization of the MWCNTs was reported elsewhere.[19−21] The solvents, dimethylformamide (DMF) and tetrahydrofuran (THF), were obtained from Fisher Scientific. PS/MWCNT nanocomposites were prepared by a solvent evaporation method. A dispersion of 5 wt % MWCNTs in DMF or THF was sonicated in an ultrasonic bath (VWR 75D) with occasional stirring. The dispersion of MWCNTs was added to a PS solution in the same solvent. The mixture was stirred and sonicated in a closed beaker alternately every 30 min for at least 6 h. As noted in an earlier work,[12] it was observed that periodic addition of solvent produced better dispersion. The nanocomposite was obtained by solvent evaporation and dried for 12−24 h in a vacuum oven at 50 °C to remove residual solvent. The dried nanocomposite was hot pressed into a disk of 2.5 cm diameter and 5 mm thickness at a temperature of 170 °C, which is above the glass transition temperature of the polymer. Samples with 0, 0.01, 0.03, 0.05, and 0.07 mass fractions of MWCNTs in PS were prepared by this method. The corresponding volume fractions were 0, 0.02, 0.05, 0.08, and 0.12 respectively. The mass fractions (w) were converted to volume fractions (β) using the simple rule of mixtures as shown in eq 1.

$$\beta = \frac{w\rho_{PS}}{\rho_{MWNCT} + w(\rho_{PS} - \rho_{MWCNT})} \quad (1)$$

Here, ρ_{PS} is the density of PS and ρ_{MWCNT} is the density of MWCNTs.

2.2. Electrical Characterization. The electrical conductivity of the nanocomposites was measured in accordance with ASTM D4496. Samples of a known cross-sectional area and thickness were placed between copper electrodes and the dc resistance was measured using an Agilent 34401A power supply. The surfaces of the sample in contact with the electrodes were coated with silver paint in order to reduce discrepancies arising from microroughness. It was ensured that the surface area of the electrodes exceeded the cross-sectional area of the disks.

2.3. Rheological Characterization. Dynamic rheological measurements were performed on a Rheometrics RDAIII rheometer using 2.5 cm parallel plates. The melt rheology was done under a nitrogen atmosphere at temperatures of 170, 180, 190, 200, and 210 °C with a gap of about 1 mm between the plates. The storage modulus, loss modulus and complex viscosity were measured as functions of frequency (0.1−100 rad/s) within the linear viscoelastic regime of the sample. Each curve reported is an average of three different samples at a given concentration.

3. Results and Discussion

3.1. Electrical Percolation in PS/MWCNT Nanocomposites. Figure 2 shows the experimentally determined electrical conductivity (σ_c) of PS/MWCNT nanocomposites, synthesized using DMF and THF, as a function of the MWCNT concentration. Each data point on the plot represents the average of measurements on 6−8 different samples, and the scatter in the data was within 5% of this average value. The conductivity of pure PS is $\sim 10^{-20}$ S/m, but adding MWCNTs increased the conductivity of the nanocomposites increased by 20 orders of magnitude, approaching a value of 1 S/m. At low concentrations of MWCNTs, closer to the onset of percolation, the nanocomposites synthesized using DMF exhibit higher electrical conductivity than those synthesized using THF. This qualitatively indicates that DMF allows better interconnectivity of MWCNTs than THF.

The conductivity data are classically interpreted by a percolation model, which gives the following power-law expression for conductivity as a function of particle volume fraction β:

$$\sigma_c^{PL} = \sigma_{PS} + A(\beta - \beta_c)^{\lambda} \quad (2)$$

Here, σ_c^{PL} is the conductivity of the nanocomposite predicted by the power-law fit, σ_{PS} is the electrical conductivity of the pure PS, A is a constant based on the interconnectivity of the MWCNTs, β_c is the percolation threshold and λ is the critical exponent. The percolation threshold corresponds to the formation of a CNT network that allows electron transport by tunneling or electron hopping along CNT interconnects. The conductivity data for PS/MWCNT nanocomposites in Figure 2 were fit using eq 2, and the fit parameters are listed in Table 1. The power-law fits to the electrical conductivity data of both the DMF and THF-processed nanocomposites yielded a normalized cross-correlation coefficient of 1.00.

From Figure 2, it can be seen that percolation begins near a volume fraction of 0.017 in the DMF-processed nanocomposites and 0.019 in the THF-processed ones. Beyond this point, there

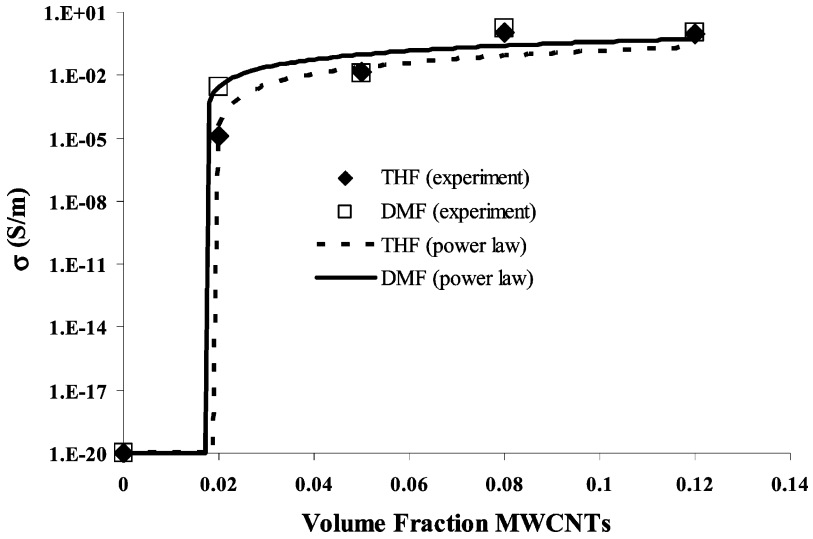

Figure 2. Electrical conductivity of the PS/MWCNT nanocomposites solvent processed using THF and DMF at various MWCNT concentrations and fits from a classical power-law. Nanocomposites processed with DMF percolate quicker than those processed with THF.

Table 1. Power Law Fit Parameters for the Electrical and Rheological Properties of the PS/MWCNT Nanocomposites Synthesized Using THF and DMF Solvents

power-law parameter	THF (σ_c)	DMF (σ_c)	THF ($\overline{\log G'}$ and $\overline{\log \eta^*}$)
A	16	16	16
β_c	0.019	0.017	0.019
λ	1.9	1.5	7

are slight differences in the percolation behavior depending on the solvent used. The nanocomposites that are solvent processed with DMF percolate more rapidly than those processed with THF as described by the critical exponents 1.5 and 1.9 respectively. However, the choice of solvent does not appear to affect the conductivity of the fully percolated nanocomposite, which in both cases is ~1 S/m. This value is reached at about 8 vol % MWNCTs. The differences in the percolation thresholds for the two solvents may indicate that DMF is a slightly better dispersant for MWCNTs than THF.

3.2. Rheological Percolation of PS/MWCNT Nanocomposites. The nanocomposites were further investigated for their dynamic rheological properties. Figures 3−6 are experimental results for the various rheological parameters obtained via dynamic melt rheology from the THF-processed PS/MWCNT nanocomposites. Parts a and b of Figure 3 are experimental results for the storage modulus, G', and the loss modulus, G'', as functions of frequency. Data collected over a temperature range of 170 to 210 °C have been shifted using the time−temperature superposition principle to extend the frequency range, and are reported at the median temperature of 190 °C. Both G' and G'' increase with MWCNT concentration. At concentrations exceeding 2 vol %, G' reaches a plateau at low frequencies indicating that the percolated MWCNTs may be forming a pseudo-solid-like network with strong interactions between polymer and particles.[22,23]

Evidence of the formation of a pseudo-solid-like network of percolated MWCNTs can also be seen in Figure 4, where the variation of G' and G'' with frequency is compared for the pure PS sample and for the nanocomposite with the highest MWCNT concentration of 12 vol %. While the pure PS melt shows a typical transition from elastic to viscous behavior ($G'' > G'$) at a critical frequency of 13 rad/s, the nanocomposite shows a predominantly elastic response ($G' > G''$, plateau in G') over the entire frequency range.

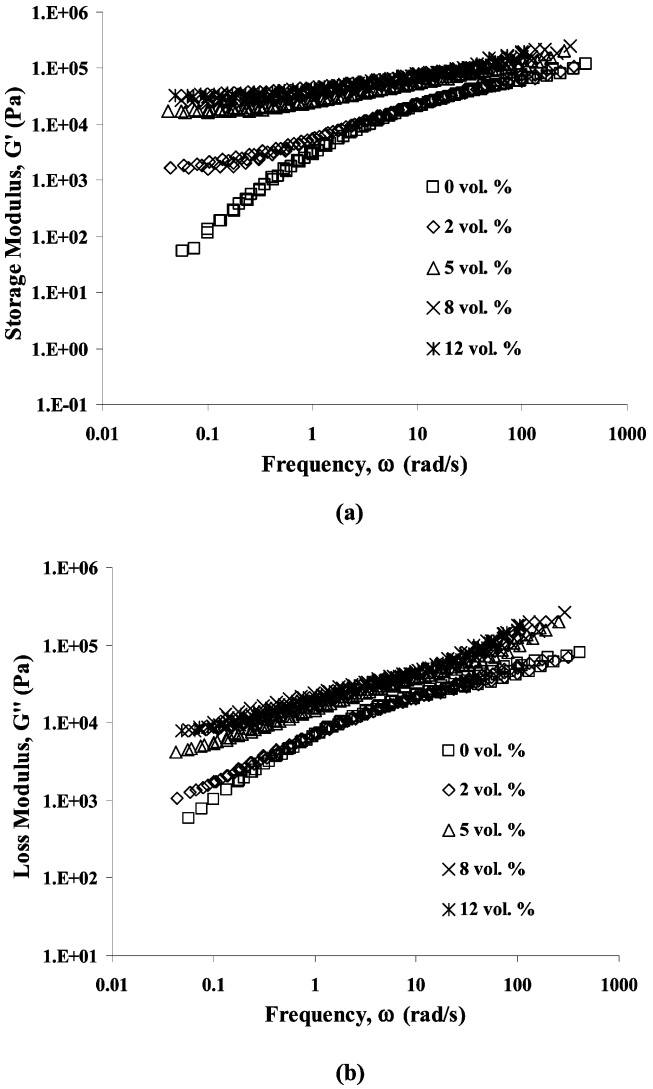

Figure 3. (a) Storage modulus (G') and (b) loss modulus (G'') of the nanocomposites as a function of frequency at a temperature of 190 °C obtained through time−temperature superposition. Data are shown for a range of MWCNT concentrations. Note the plateau in G' at low frequencies for all of the MWCNT concentrations indicating the presence of a pseudo-solid-like network in the nanocomposite formed by the percolation of MWCNTs.

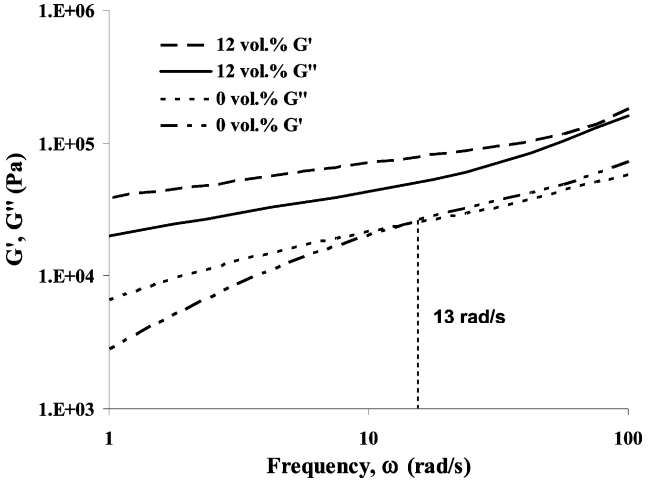

Figure 4. Crossover point of the G' and G'' curves for the pure PS and the 12 vol % MWCNT nanocomposites. While the pure PS shows a viscous response at lower frequencies, the 12 vol % MWCNT nanocomposite shows a predominantly elastic response over the entire frequency range.

Differences in rheological response upon addition of MWCNTs can also be noted in the complex viscosity, η^*. From the frequency dependence of η^* in Figure 5a, it can be seen that the pure PS melt shows a Newtonian plateau in η^* at low frequencies. On the other hand, the nonzero MWCNT concentrations do not show a plateau over the frequency range, indicative of elastic behavior in the PS/MWCNT nanocomposites due to interactions between the MWCNTs. As the concentration of MWCNTs increases, a percolated network forms and the nanocomposite develops a finite yield behavior. Correspondingly, a plot of η^* vs the complex modulus, G^*, exhibits divergence at concentrations above 2 vol %, as shown in Figure 5b.[24] The asymptotic complex modulus increases from 13800 Pa at an MWCNT concentration of 5 vol % to 30 300 Pa at 12 vol %. In addition, while pure PS exhibits a plateau in complex viscosity in the low complex modulus regime, the diverging curves of PS/MWCNT nanocomposites exhibit complex viscosity plateaus, ranging from 1700 Pa s at 5 vol % to 2400 Pa s at 12 vol %, in the high complex modulus regime.

Additional insight into the interaction between the MWCNTs and the PS matrix can be obtained from the inverse loss tangent, G'/G'', which is a measure of the damping characteristics or firmness of the material.[10,17] As shown in Figure 6, the inverse loss tangent increases with MWCNT concentration, especially at low frequencies. This indicates a hindrance to energy dissipation and relaxation of the polymer chains due to the percolation of the MWCNTs.

3.3. Comparison of Electrical and Rheological Percolation. A closer examination of the low frequency (0.1 rad/s) regime in Figures 2−5, indicates an increase in all the rheological parameters with MWCNT concentration for the THF-processed nanocomposites. As expected from previous research investigations,[7,25] the parameter whose absolute values are most sensitive to particle concentration is the storage modulus G', which increased by more than 2 orders of magnitude upon adding MWCNTs. Over the same range of MWCNT concentrations, the absolute values of η^*, G'', and G'/G'' each increased by about an order of magnitude.

Similar to the electrical percolation threshold, rheological percolation threshold is correlated with the onset of power-law dependence of a rheological property on the volume fraction. However, there is no agreement on which quantity to use in this regard: for example, while Du et al.[11] report the percolation based on G', Kharchenko et al.[17] report the percolation based on G'/G''. In order to understand which rheological parameter describes percolation better, the normalized−log values of various directly measured, $\log G'$ and $\log G''$, and derived

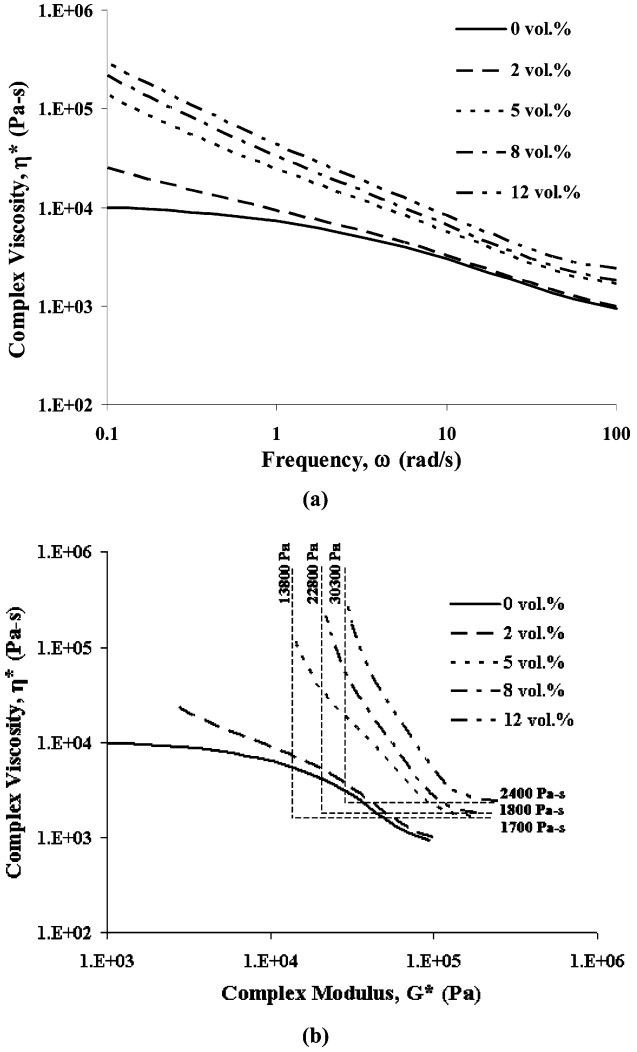

Figure 5. Complex viscosity (η^*) as a function of **(a)** frequency (ω), and **(b)** complex modulus (G^*) for the PS/MWCNT nanocomposites processed with THF and tested at a temperature of 190 °C. Data are shown for a range of MWCNT concentrations. Note the plateau in complex viscosity in the high complex modulus regime.

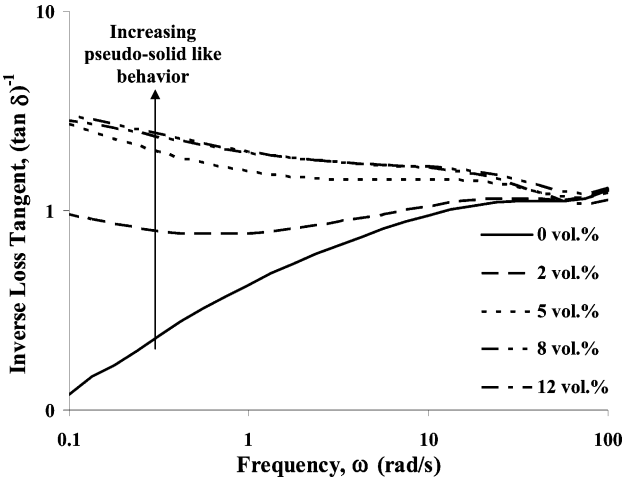

Figure 6. Inverse loss tangent as a function of frequency. Note the increase in inverse loss tangent with MWCNT concentration.

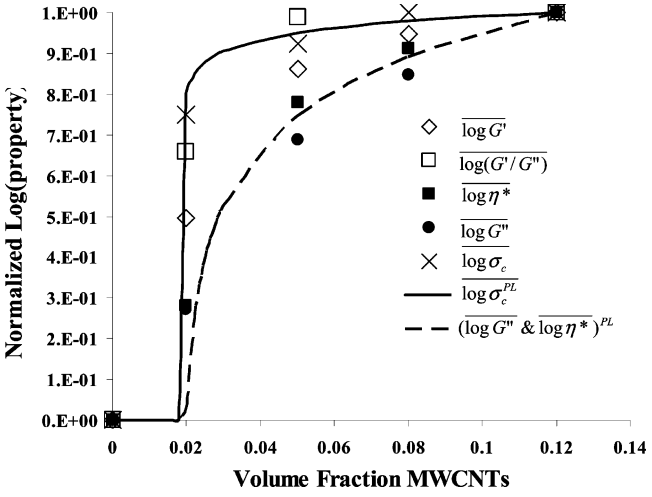

Figure 7. The log-normalized values of storage modulus ($\overline{\log G'}$), loss modulus ($\log G''$), complex viscosity ($\overline{\log \eta^*}$), inverse loss tangent ($\overline{\log(G'/G'')}$), electrical conductivity ($\overline{\log \sigma_c}$) and the power law fit for electrical conductivity ($\log \sigma_c^{PL}$) as a function of the MWCNT concentration at 190 °C for THF-processed nanocomposites. The rheological data were obtained from Figures 2, 4, and 5 at a frequency of 0.1 rad/s. The viscous rheological parameters, G'' and η^*, exhibit a gradual percolation rate, and hence a modified power-law fit (($\overline{\log G''}$ and $\overline{\log \eta^*})^{PL}$) was used.

Table 2. Normalized Cross-Correlation Values for the Normalized Logarithm of Rheological Parameters for PS/MWCNT Nanocomposites Processed with THF Solvent When Compared with the Normalized Logarithm of the Power-Law Fits to the Electrical Conductivity Measurements for THF Processed PS/MWCNT Nanocomposites and the Fits to $\log G''$ and $\log \eta^*$ in Figure 6

rheological parameter	power-law ($\log \sigma_c^{PL}$)	power-law ($\log G''$ and $\log \eta^*$)
G'	0.95	0.92
G'/G''	0.98	0.84
G''	0.86	0.97
η^*	0.87	0.98

rheological parameters, $\overline{\log \eta^*}$ and $\overline{\log(G'/G')}$, are plotted in Figure 7, and compared with the normalized−log values of electrical conductivity, $\overline{\log \sigma_c}$, and the power-law predictions of electrical conductivity, $\log \sigma_c^{PL}$. In addition, a power law of the form described by eq 2 was used to fit the G'' and η^* data (fit parameters reported in Table 1 alongside the parameters for the electrical conductivity data) and the normalized log values of the modified power-law predictions,($\overline{\log G''}$and $\overline{\log \eta^*})^{PL}$, are also plotted in Figure 7.

An inspection of Figure 7 reveals that $\overline{\log G''}$ and $\overline{\log \eta^*}$ exhibit a percolation behavior that is far more gradual when compared to $\overline{\log G'}$ and $\overline{\log G'/G''}$ and $\overline{\log \sigma_c}$. Quantitative comparisons between fits were made using normalized cross-correlation coefficient values (Table 2). Both $\overline{\log G''}$ and $\overline{\log \eta^*}$ seem to match well with ($\overline{\log G''}$ and $\overline{\log \eta^*})^{PL}$ yielding normalized cross-correlation coefficients of 0.97 and 0.98 respectively, as opposed to 0.86 and 0.87 respectively when compared with $\log \sigma_c^{PL}$. At lower concentrations of MWCNTs, closer to the electrical percolation threshold, $\overline{\log G'/G''}$ matches better with $\overline{\log \sigma_c^{PL}}$ when compared to$\overline{\log G'}$. At higher concentrations, both $\overline{\log G'}$ and $\overline{\log G'/G''}$ match well with $\overline{\log \sigma_c^{PL}}$. Overall, comparing $\overline{\log G'}$ and $\overline{\log G'/G''}$ with $\log \sigma_c^{PL}$ yielded normalized cross-correlation coefficients of 0.95 and 0.98 respectively, as opposed to 0.92 and 0.84 respectively when compared with ($\overline{\log G''}$ and $\overline{\log \eta^*})^{PL}$.

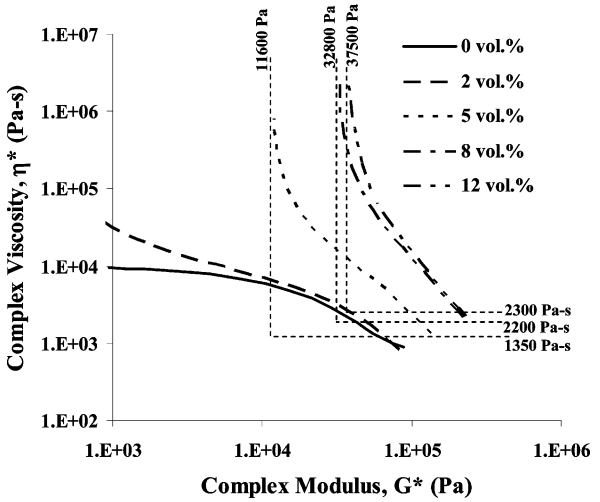

Figure 8. Complex viscosity (η^*) as a function of complex modulus (G^*) for the PS/MWCNT nanocomposites processed with DMF and tested at a temperature of 190 °C. Data are shown for a range of MWCNT concentrations. Note the plateau in complex viscosity in the high complex modulus regime.

It can be noted that while G' and G'' are directly measured rheological parameters, η^* and G'/G'' are derived rheological parameters that have physical significance in terms of the flow and firmness of the nanocomposites. From Figure 7, it can be concluded that to report percolation, G' is a good choice among the directly measured rheological parameters, and G'/G'' is a good choice among the derived rheological parameters due to the steep increase in their values at low MWCNT concentrations. Microstructurally, this indicates that the elastic load transfer and electrical conductivity are far more sensitive to the onset of percolated MWCNTs than the viscous dissipation mechanisms as quantified by the change in the power-law exponent.

3.4. Effect of Solvent on the Rheological Percolation. In order to study the influence of solvent on rheological percolation, the variation of η^* with G^* obtained from the DMF-processed nanocomposites (Figure 8) was compared with that results obtained from the THF-processed nanocomposites (Figure 5b). In Figure 8, the asymptotic complex modulus increases from 11600 Pa at 5 vol % MWCNTs to 37 500 Pa at 12 vol %. Comparing with Figure 5b, the G^* value at 12 vol % is 25% greater for the DMF-processed nanocomposites as compared to the THF ones. The diverging curves of the DMF-processed nanocomposites exhibit complex viscosity plateaus similar to those observed with THF ones and their values range from 1350 Pa s at an MWCNT concentration of 5 vol % to 2300 Pa s at 12 vol %. However, the complex viscosity plateau for the fully percolated (12 vol %) nanocomposites does not vary significantly with the choice of solvent.

Next, the normalized log values of various rheological parameters and electrical conductivity obtained from the DMF-processed nanocomposites (Figure 9) were compared with the results obtained from the THF-processed nanocomposites (Figure 7) using the normalized cross-correlation coefficients (Table 3). Figure 9 reveals that in DMF-processed nanocomposites, $\overline{\log G''}$ and $\overline{\log \eta^*}$ exhibit a percolation behavior that is more gradual when compared with $\overline{\log G'}$, $\overline{\log G'/G''}$ and $\overline{\log \sigma_c^{PL}}$. Both $\overline{\log G''}$ and $\overline{\log \eta^*}$ appear to correlate well with ($\overline{\log G''}$ and $\overline{\log \eta^*})^{PL}$, yielding normalized cross-correlation

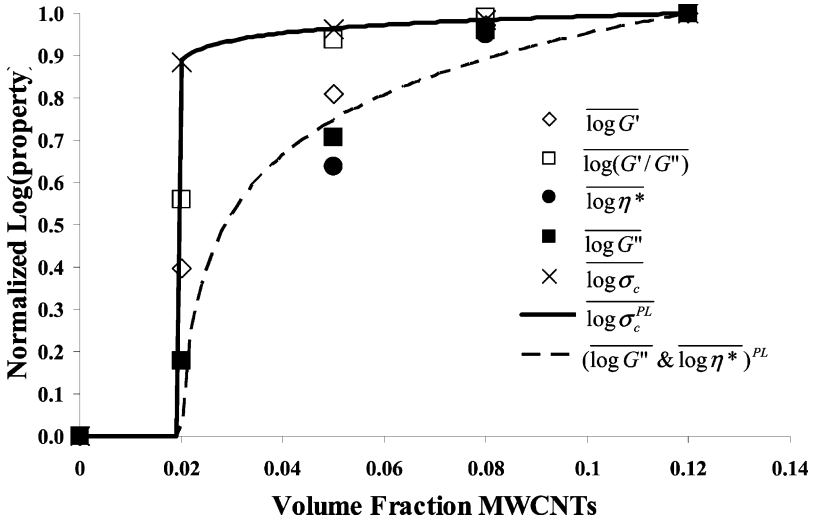

Figure 9. The log−normalized values of storage modulus ($\overline{\log G'}$), loss modulus ($\overline{\log G''}$), complex viscosity ($\overline{\log \eta^*}$) and inverse loss tangent ($\overline{\log(G'/G'')}$), electrical conductivity ($\overline{\log \sigma_c}$) and the power law fit for electrical conductivity ($\overline{\log \sigma_c^{PL}}$) as a function of the MWCNT concentration at 190 °C for DMF-processed nanocomposites. The rheological data was obtained at a frequency of 0.1 rad/s. Note that η^* and G'' percolate similar to that predicted by the modified power-law ($(\overline{\log G''}$ and $\overline{\log \eta^*})^{PL}$) for THF-processed nanocomposites. However, G' and G'/G'' percolate more gradually compared to σ_c. This is in contrast to that observed with the THF-processed nanocomposites.

Table 3. Normalized Cross-Correlation Values for the Normalized Logarithm of Rheological Parameters for PS/MWCNT Nanocomposites Processed with DMF Solvent When Compared with the Normalized Logarithm of the Power-Law Fits to the Electrical Conductivity Measurements for DMF Processed PS/MWCNT Nanocomposites and the Fits to $\overline{\log G''}$ and $\overline{\log \eta^*}$ in Figure 6

rheological parameter	power-law ($\overline{\log \sigma_c^{PL}}$)	power-law ($\overline{\log G''}$ and $>\overline{\log \eta^*}$)
G'	0.88	0.95
G'/G'	0.94	0.89
G''	0.76	0.98
η^*	0.77	0.99

coefficients of 0.98 and 0.99 respectively, as opposed to 0.76 and 0.77 respectively when compared with $\log\sigma_c^{PL}$. This behavior is similar to that observed in the THF-processed nanocomposites. However, in the DMF-processed nanocomposites, unlike the THF-processed ones, both $\overline{\log G'}$ and $\overline{\log G'/G''}$ increase more gradually when compared with $\log\sigma_c^{PL}$ yielding normalized cross-correlation coefficients of 0.88 and 0.94 respectively, as opposed to 0.95 and 0.89 respectively when compared with ($\overline{\log G''}$ and $\overline{\log \eta^*}$)^{PL}. This indicates that DMF influences the electrical conductivity more than the elastic behavior of the nanocomposites. All of these results are consistent with previous investigations into the effects of these solvents on the electrospinning of PS, where the conductivity of PS solutions with DMF was found to be 2.4 μS/cm, compared to ~0 μS/cm with THF, and the surface tension was found to be 34.339 mN/m, compared to 24.735 with THF.[2]

4. Conclusions

In this systematic investigation, the influence of adding multiwalled carbon nanotubes (MWCNTs) filler to a commercial polydispersed polystyrene (PS) on the electrical and rheological behavior of the resulting nanocomposite was studied. The power law fits to the electrical conductivity measurements indicate that the microstructure starts to percolate at 1 vol %. In comparison to the pure PS, the conductivity increased by 20 orders of magnitude to a value of 1 S/m at 8 vol %. Significant enhancements were also observed in rheological parameters with increasing MWCNT concentration. The storage modulus exhibited a low-frequency plateau at concentrations exceeding 2 vol % that suggests the formation of a pseudo-solid-like network of percolated MWCNTs.

By quantitatively comparing the normalized log values of electrical conductivity and various rheological parameters across the concentrations of interest, it was concluded that η^* and G'' are less sensitive to percolation when compared to G', G'/G'', and σ_c. Microstructurally, this indicates that the elastic load transfer and electrical conductivity are far more sensitive to the onset of percolated MWCNTs than the dissipation mechanisms that affect the viscous response.

The electrical and rheological percolations also exhibit sensitivity to the choice of solvent. DMF imparts higher electrical percolation at lower concentrations of MWCNTs when compared with THF. In a fully percolated microstructure, it was also observed that complex modulus of DMF-processed nanocomposites was 25% higher when compared with THF. While the variation of the normalized electrical conductivity and rheological parameters with MWCNT concentration in DMF-processed nanocomposites indicate similar sensitivity as observed in the THF-processed nanocomposites, DMF influences the electrical conductivity more than the elastic behavior of the nanocomposites.

Acknowledgment. This work was supported by NASA-Goddard Space Flight Center and by ONR award number N000140710391.

References and Notes

(1) Andrews, R.; Jacques, D.; Minot, M.; Rantell, T. *Macromol. Mater. Eng.* **2002**, *287*, 395.
(2) Xheng, J.; He, A.; Li, J.; Xu, J.; Han, C. C. *Polymer* **2006**, *47*, 7095.
(3) Qian, D.; Dickey, E. C. *J. Microsc.* **2001**, *204*, 39.
(4) Qian, D.; Dickey, E. C. *Appl. Phys. Lett.* **2002**, *76*, 2868.
(5) Thostenson, E. T.; Chou, T.-W. *J. Phys. D Appl. Phys.* **2002**, *35*, L77.
(6) Safadi, B.; Andrews, R.; Grulke, E. A. *J. Appl. Polym. Sci.* **2001**, *84*, 2260.
(7) Mitchell, C. A.; Bahr, J. L.; Arepalli, S.; Tour, J. M.; Krishnamoorti, R. *Macromolecules* **2002**, *35*, 8825.
(8) Potschke, P.; Brunig, H.; Janke, A.; Fischer, D.; Jehnichen, D. *Polymer* **2005**, *46*, 10355.
(9) Potschke, P.; Fornes, T. D.; Paul, D. R. *Polymer* **2002**, *43*, 3247.

(10) McNally, T.; Potschke, P.; Halley, P.; Murphy, M.; Martin, D.; Bell, S. E. J.; Brennan, G. P.; Bein, D.; Lemoine, P.; Quinn, J. P. *Polymer* **2005**, *46*, 8222.
(11) Du, F.; Scogna, R. C.; Zhou, W.; Brand, S.; Fischer, J. E.; Winey, K. I. *Macromolecules* **2004**, *37*, 9048.
(12) Bryning, M. B.; Islam, M. F.; Kikkawa, J. M.; Yodh, A. G. *Adv. Mater.* **2005**, *17*, 1186.
(13) Ramasubramaniam, R.; Chen, J. *Appl. Phys. Lett.* **2003**, *83*, 2928.
(14) Sandler, J. K. W.; Kirk, J. E.; Kinloch, I. A.; Shaffer, M. S. P.; Windle, A. H. *Polymer* **2003**, *44*, 5893.
(15) Wu, G.; Lin, J.; Zheng, Q.; Zhang, M. *Polymer* **2006**, *47*, 2442.
(16) Potschke, P.; Abdel-Goad, M.; Alig, I.; Dudkin, S.; Lellinger, D. *Polymer* **2004**, *45*, 8863.
(17) Kharchenko, S. B.; Douglas, J. F.; Obrzut, J.; Grulke, E. A.; Migler, K. B. *Nat. Mater.* **2004**, *3*, 564.
(18) Hines, P. J.; Duckett, A.; Read, D. J. *Macromolecules* **2007**, *40*, 2782.
(19) Andrews, R.; Jacques, D.; Rao, A. M.; Derbyshire, F.; Qian, D.; Fan, X.; Dickey, E. C.; Chen, J. *Chem. Phys. Lett.* **1999**, *303*, 467.
(20) Andrews, R.; Jacques, D.; Qian, D.; Dickey, E. C. *Carbon* **2001**, *39*, 1681.
(21) Bom, D.; Andrews, R.; Jacques, D.; Anthony, J.; Chen, B.; Meier, M. S.; Selegue, J. P. *Nano Lett.* **2002**, *2*, 615.
(22) Krishnamoorti, R.; Giannelis, E. P. *Macromolecules* **1997**, *30*, 4097.
(23) Agarwal, S.; Salovey, R. *Polym. Eng. Sci.* **1995**, *35*, 1241.
(24) Enikolopyan, N. S.; Fridman, M. L.; Stalnova, I. O.; Popov, V. L. *Adv. Polym. Sci.* **1990**, *96*, 1.
(25) Mackay, M. E.; Dao, T. T.; Tuteja, A.; Ho, D. L.; Horn, B. V.; Kim, H.-C.; Hawker, C. J. *Nat. Mater.* **2003**, *2*, 762.

MA0711792